

Detection of confinement and jumps in single-molecule membrane trajectories

N. Meilhac,¹ L. Le Guyader,² L. Salomé,² and N. Destainville¹

¹Laboratoire de Physique Théorique, UMR CNRS-UPS 5152, Université Paul Sabatier, 31062 Toulouse Cedex 9, France

²Institut de Pharmacologie et de Biologie Structurale, UMR CNRS-UPS 5089, 205, route de Narbonne, 31077 Toulouse Cedex, France

(Received 20 July 2005; published 26 January 2006)

We propose a variant of the algorithm by [R. Simson, E. D. Sheets, and K. Jacobson, *Biophys.* **69**, 989 (1995)]. Their algorithm was developed to detect transient confinement zones in experimental single-particle tracking trajectories of diffusing membrane proteins or lipids. We show that our algorithm is able to detect confinement in a wider class of confining potential shapes than that of Simson *et al.* Furthermore, it enables to detect not only temporary confinement but also *jumps* between confinement zones. Jumps are predicted by membrane skeleton fence and picket models. In the case of experimental trajectories of μ -opioid receptors, which belong to the family of G-protein-coupled receptors involved in a signal transduction pathway, this algorithm confirms that confinement cannot be explained solely by rigid fences.

DOI: [10.1103/PhysRevE.73.011915](https://doi.org/10.1103/PhysRevE.73.011915)

PACS number(s): 87.16.-b

One of the central issues of contemporary cellular biology is to establish the relationship between dynamical organization and biological functions of membrane constituents. The development of single-particle tracking (SPT) techniques gives insight into dynamical organization of membranes that have been inaccessible by ensemble-average methods. Indeed, the diffusive motion of molecules of interest (proteins or lipids) at the surface of living cells can be followed with a nanometric resolution, after labeling them by means of fluorophores, gold colloids, latex beads, or quantum dots [1]. Yet, specific and performant tools must be developed to extract valuable information from these trajectories.

After more than 15 years of efforts using SPT techniques, the question of cell membrane organization and compartmentalization is still a matter of intense and controversial debate [2–7]. What is the origin of the confinement quite generally observed in tracking experiments? How is it related to the transmission of signals through the membrane? Confinement is, indeed, commonly observed in SPT trajectories: the diffusive motion is not purely Brownian, but rather affected by either rigid obstacles [confining domains such as rafts (or other signaling platforms)] or molecular interactions. Confinement can be transient [2], the molecule being now and then trapped in “transient confinement zones” (TCZs). Experimental situations also exist where the molecule is always confined, while showing a long-term slow diffusion. There exist different models that account for such a behavior. In the “membrane skeleton fence and picket models” [8,9], the confinement is due to the cytoskeleton of the cell close to the membrane, or by proteins anchored to it, which form rigid corrals. Successive hops between adjacent domains result in a slow long-term diffusion of the molecules (Fig. 1). The recent alternative “interacting Brownian particle model” [4] proposes that, in the case studied in this reference, barriers do not satisfyingly explain the observed confinement, which more likely originates from long-range attractive interactions between membrane proteins. The latter form autoassembled aggregates in which proteins are trapped. The long-term diffusive behavior is the manifestation of the diffusion of the center of mass of the assembly. We demonstrate that the algorithm studied in this paper is

able to discriminate between these models. Indeed, in a fence and picket model, proteins regularly jump from a confining zone to an adjacent one. By contrast, the “interacting Brownian particle model” does not require jumps to account for long-term slow diffusion. We show that, despite statistical fluctuations, our algorithm detects jumps with good confidence, when they exist. We calculate how many jumps are theoretically expected in a fence and picket model and compare this number to the effectively detected ones in experimental trajectories of Ref. [4] (μ -opioid receptors). We find that there is an unequivocal discrepancy. This proves that rigid fences cannot be considered as a unique source of confinement.

Beyond this particular example, our algorithm intends to be applicable to a wide range of experimental situations. It responds to an increasing demand consecutive to the rapid development of SPT experiments. It is a challenge to develop a simple and reliable tool to discriminate between different sources of confinement or, more simply, between confined

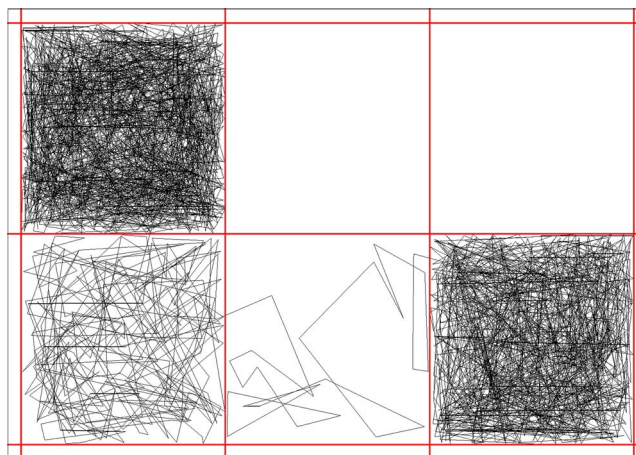


FIG. 1. (Color online) Example of trajectory in a square grid of rigid barriers of periodicity L . At short times, the particle diffuses in a closed box, where it stays on average a time τ_{res} . Periodically, it jumps from one box to an adjacent one, thus, resulting in a slow long-term diffusion with constant D_M .

and nonconfined trajectories. The present paper intends to propose such a robust tool.

Simson *et al.*'s algorithm [10] has been designed to detect transient confinement. It is based on the following principle. Consider a Brownian trajectory $\mathbf{r}(t)$ on a time interval $[t_0, t_0 + \delta t]$. The maximum of $\|\mathbf{r}(t) - \mathbf{r}(t_0)\|^2$ on $[t_0, t_0 + \delta t]$, denoted by r_{\max}^2 , scales like $D\delta t$, where D is the diffusion constant. Then the authors define a confinement index λ (denoted by L in their paper) that is an affine function of $D\delta t/r_{\max}^2$. D is determined by measuring the slope at the origin of the mean-square deviation (MSD), $\text{MSD}(t)$. If the diffusion is confined in a domain of typical size L , then r_{\max}^2 is limited by L^2 , and λ is larger than in the case of free Brownian diffusion. The authors determine a threshold λ_c . Roughly speaking, if $\lambda > \lambda_c$, the diffusion is confined; otherwise, it is free (see Ref. [10] for more details). Along a trajectory, $\lambda(t)$ is calculated on sliding intervals $[t - \delta t/2, t + \delta t/2]$. The plot of $\lambda(t)$ indicates TCZs as intervals where $\lambda > \lambda_c$.

We show that even though Simson *et al.*'s method is applicable to a large variety of experimental cases, there exist situations of great interest where it is not operational. First, artifactual detections of TCZs can happen when D varies along the trajectory [4]. This problem is fixed by computing D locally by the same method, on intervals of a few seconds. More importantly, this method fails in detecting confinement in nonflat potentials. For example, in a quadratic well of typical width L at temperature T , the molecule is likely to explore regions of energy of several $k_B T$ where $r \gg L$, and the measured r_{\max}^2 fluctuates a lot around its typical value, depending on whether or not such rare points are in the trajectory. We experienced that it happens that Simson *et al.*'s algorithm does *not* detect flagrant confinement in quadratic potentials or in experimental trajectories (see Fig. 2, for example). The algorithm proposed in Ref. [11], also based on r_{\max}^2 , presents the same limitations. This is intrinsic to the methods, namely, the choice of r_{\max}^2 to characterize trajectory wanders, and not to a particular choice of parameters.

For this reason, we modify the above algorithm as follows: instead of calculating r_{\max}^2 , we compute the variance $\Delta r^2(t)$ of \mathbf{r} on intervals $[t - \delta t/2, t + \delta t/2]$. Rare points wandering far away from the potential minimum thus have a low weight in $\Delta r^2(t)$, which gives a more accurate measurement of the typical width of the confining potential. Of course, in the case of flat potentials delimited by rigid fences, both algorithms present a similar efficiency. A confinement index is now defined

$$\Lambda = \frac{D\delta t}{\Delta r^2}. \quad (1)$$

Up to a numerical prefactor, Λ is the ratio of the variance of a free random walk to the variance of the trajectory under study. If it is unconfined, Λ will be of order unity, whereas it will be large in the converse case. We calculate the typical values of Λ in the respective cases of free Brownian two-dimensional trajectories and confined ones. We model our Brownian molecule by an overdamped Langevin particle: $d\mathbf{r}/dt = \boldsymbol{\eta}(t)$, where $\boldsymbol{\eta}$ is a Gaussian white noise: $\langle \boldsymbol{\eta} \rangle = \mathbf{0}$

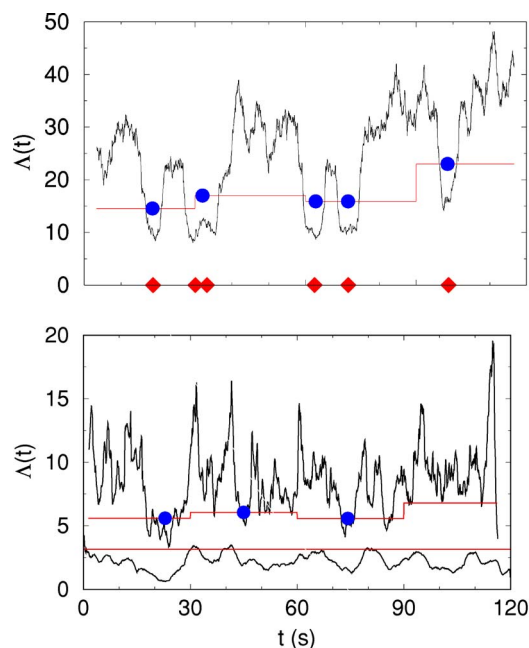


FIG. 2. (Color online) Top: Profile $\Lambda(t)$ for a numerical trajectory with $\tau_{\text{res}} = 20$ s. We have also plotted the threshold $\alpha\bar{\Lambda}(t)$ with $\alpha = 0.7$. Real jumps are represented by diamonds and detected ones by circles. One can see five detected jumps among which there is one double jump (detected only once). Note that the first and last $\delta t/2$ segments are not taken into account because $\Lambda(t)$ cannot be calculated there. Bottom (upper plot): Profile for an experimental trajectory, with three detected jumps. Here $\tau_{\text{res}} = 9.6$ s and the fence model would predict 12 jumps. Some intervals where $\Lambda(t) \leq \alpha\bar{\Lambda}(t)$ are not considered as jumps because they are not long enough. Bottom (lower plot): Profile $\lambda(t)$ calculated with Simson *et al.*'s algorithm [10] and the threshold $\lambda_c = 3.16$ (see [10] for details). The receptor is apparently hardly ever confined.

$\langle \eta_i(t) \eta_j(t') \rangle = 2D \delta_{ij} \delta(t - t')$. Then the mean position $\bar{\mathbf{r}}$ and the mean-square position \bar{r}^2 are calculated on a *single* trajectory before being averaged over noise, leading to $\Delta r^2 = \langle \bar{r}^2 - \bar{r}^2 \rangle = \binom{2}{3} D \delta t$. Statistical fluctuations of this quantity can also be calculated using Wick's theorem [12] to compute four-time correlators of $\boldsymbol{\eta}$: $\Delta \langle \bar{r}^2 - \bar{r}^2 \rangle = \frac{2\sqrt{2}}{3\sqrt{5}} D \delta t$. Thus, $\Lambda_{\text{Brown}} \leq 1 / \left(\frac{2}{3} - \frac{2\sqrt{2}}{3\sqrt{5}} \right) \approx 4$ for a pure Brownian trajectory, independently of δt and D , as checked on numerical trajectories. Now we consider confined diffusion in a square box of side L . If one averages over $N \gg 1$ independent positions, one gets $\Delta r^2 = L^2/6$,

$$\Lambda_{\text{conf}} = 6D\delta t/L^2. \quad (2)$$

In this confined case, the statistical fluctuations of Δr^2 vanish at large N . Hence TCZs will be distinguishable from pure Brownian trajectories if $\Lambda_{\text{conf}} \gg \Lambda_{\text{Brown}}$, i.e., if $\Lambda_{\text{conf}} \gg 4$ or $D\delta t/L^2 \gg \frac{2}{3}$. As expected, δt must be sufficiently large to enable detection. Note that above we have asked for the number of *independent* images to be sufficiently large. In practice, positions in successive images *are* correlated because the equilibration time to explore a box of side L is τ

$=L^2/\pi^2D$ [4]. One must make sure that $N \gg 1$ with respect to this time.

Our algorithm detects confinement with excellent reliability, whatever the shape of the box or of any nonflat confining potential. Now how does it detect jumps over fences? We suppose, first, that the molecule evolves in a grid of square boxes of side L , separated by rigid barriers, and that it can jump over a barrier by thermal activation (Fig. 1). It has a long-term slow diffusion with a constant D_M : $\Delta r^2 = 4D_M t$ at large t . If τ_{res} is the average time of residence in a box (i.e., the average time between successive jumps), then $L^2 = 4D_M \tau_{\text{res}}$. When the molecule is confined in a single box, $\Lambda = \Lambda_{\text{conf}}$. If there is a jump at time t_0 in a segment $I = [t - \delta t/2, t + \delta t/2]$, then the particle is virtually in a larger box $2L \times L$; it spends a time $t_0 - t + \delta t/2$ in a box and the remaining time in an adjacent one. If $\delta t \gg \tau$, the probability distribution of the molecule position is close to uniform in each box. This permits to calculate Δr^2 by partitioning I in two intervals, one for each box. One gets

$$\Lambda(t) = \frac{2}{5} \frac{\Lambda_{\text{conf}}}{1 - \frac{12(t-t_0)^2}{5\delta t^2}} < \Lambda_{\text{conf}}. \quad (3)$$

There is a gap centered at t_0 in the profile $\Lambda(t)$ and $\Lambda(t_0) = 2\Lambda_{\text{conf}}/5$ (see Fig. 2). In the case of multiple jumps in I , the corresponding gaps merge. To resolve single jumps at best, we choose $\delta t \leq \tau_{\text{res}}/3$. In addition, δt must be as large as possible to get higher profiles $\Lambda(t)$ where confinement is best detected. Therefore, we set

$$\delta t = \frac{1}{3} \tau_{\text{res}} = \frac{L^2}{12D_M}. \quad (4)$$

In order to detect these gaps, one must also make sure that their minima are higher than Λ_{Brown} , the ‘‘background noise’’ of pure Brownian trajectories. Indeed, if not, the depth of the gap will be reduced, and this will corrupt detection. This condition reads $2\Lambda_{\text{conf}}/5 > 4$, or $\Lambda_{\text{conf}} > 10$. Together with Eq. (4), it can be written in terms of the measurable quantities D and D_M

$$D > 20D_M. \quad (5)$$

In other words, long- and short-term time scales must be well separated. This is observed in a large majority of the experimental trajectories below.

Now we evaluate the capabilities of our algorithm on numerical trajectories. They simulate Brownian molecules evolving in a square grid of rigid barriers of periodicity L . When a step crosses a barrier, it is allowed with a probability p suitably defined so that the long-term diffusion constant equals D_M . Numerical parameters match those of experimental trajectories (see below). One image is sampled every 40 ms. In addition, D is allowed to vary slowly with time in a given trajectory, to mimic possible composition or physical changes of the underlying membrane. More precisely, every second, D is multiplied by a factor randomly chosen in the interval $[0.9, 1.1]$. To calculate Λ , we *measure* the diffusion constant D_m by calculating the MSD on intervals of 5 s and fitting the slope at the origin (first three points). We check

that $D_m \simeq D$. Because of statistical fluctuations on finite samples, all jumps cannot be detected and there are false detections. We denote by σ the fraction of jumps successfully detected by the algorithm among real jumps and by $\bar{\sigma}$ the ratio of false detections to real jumps. The higher σ and the lower $\bar{\sigma}$ are, the best the algorithm. To localize jumps, we need to estimate the value Λ_{conf} since gaps are intervals where $\Lambda(t)$ is significantly smaller than the confinement value Λ_{conf} for a sufficient duration. In practice, we proceed as follows. We compute D_m as detailed above. We measure Δr^2 and we calculate $\Lambda(t)$ (see Fig. 2). To avoid biases due to the slow variations of D , we calculate the average $\bar{\Lambda}(t)$ of $\Lambda(t)$ over successive segments of 30 s; $\bar{\Lambda}(t)$ is our estimation of the confined profile: $\bar{\Lambda}(t) \simeq \Lambda_{\text{conf}}$, because we anticipate that jumps are rare. Next, we detect intervals where the signal is well below $\bar{\Lambda}$. More precisely, we require that $\Lambda(t) \leq \alpha \bar{\Lambda}(t)$ for a duration larger than t_c , where the parameters t_c and $\alpha \in [0, 1]$ must be optimized. We have scanned large ranges of values of both α and t_c , and calculated σ and $\bar{\sigma}$ in each case (10^3 trajectories of $T=120$ s), with the typical parameters of the experimental trajectories below: $D \simeq 0.1 \mu\text{m}^2 \text{s}^{-1}$, $L \simeq 0.3 \mu\text{m}$, $\tau_{\text{res}} = 10\text{--}20$ s. We observed that $t_c = \delta t/2$ and $\alpha = 0.7$ gives the best compromise with $\sigma \geq 63\%$ and $\bar{\sigma} \leq 0.7\%$. The algorithm detects two-thirds of the jumps and makes very few false detections. The value of σ comes from the fact that close jumps cannot be resolved and are counted only once.

Another serious complication can arise in experimental trajectories. The confinement domains are not necessarily squares. If they are elongated, like rectangles or more complex shapes, Eq. (3) is no longer valid. Consider, for instance, rectangles $L \times \rho L$. There are two types of jumps, over short or long edges. It can easily be quantified how this affects the relative depths of the gaps associated with each type of jump. If the rectangle is extremely elongated, then only jumps over short edges can be reasonably detected. This complication can be overcome by measuring Δx^2 and Δy^2 and multiplying the latter by a counterweight: $\Delta_{\text{cw}} r^2 = \Delta x^2 + \Delta y^2/\rho^2$. Then both kinds of gaps again have the same depth and the previous analysis becomes valid. If the main axis of the box are not parallel to the axes Ox and Oy , then before applying counterweights, one must recover the average directions of these main axes by diagonalizing the correlation matrix $C = \langle \mathbf{r}(t)\mathbf{r}^T(t) \rangle - \langle \mathbf{r}(t) \rangle \langle \mathbf{r}^T(t) \rangle$ averaged over sufficiently long time intervals (typically 30 s). We checked that this procedure is operational, even though it significantly increases the number of false detections because of additional numerical operations. However, this question goes beyond the scope of this paper because in the experimental trajectories below, by diagonalizing C , we find $\rho \simeq 1.4$ on average (while $\rho \simeq 2.1$ for a pure unconfined random walk [13]), in which case both types of gaps have typically the same depth and σ and $\bar{\sigma}$ are not significantly affected if one uses the original profile (1): $\sigma \geq 55\%$ and $\bar{\sigma} \leq 2.5\%$.

Now we apply our algorithm to the 102 experimental trajectories from Ref. [4]. These are trajectories of μ -opioid receptors at the surface of normal rat kidney fibroblast cells, tracked by SPT, after being labeled by 40 nm gold colloids,

at 40 ms time resolution during $T=120$ s. The parameters D , D_M , and L are measured [4] by fitting the MSD by $\text{MSD}(t) = (L^2/3)[1 - \exp(-12Dt/L^2)] + 4D_M t$. Typically, $D \sim 0.1 \mu\text{m}^2 \text{s}^{-1}$, $L \sim 0.3 \mu\text{m}$, $\tau_{\text{res}} \sim 10$ s. From D_M and L , we deduce τ_{res} . In [4], it was noted that $\sim 15\%$ of the trajectories show significant slow variations of D and L^2 in a same trajectory, up to one order of magnitude for D . This could be a serious concern because variations of these parameters cause variations of the reference value Λ_{conf} that could be misinterpreted as jumps. Fortunately, it was also noted that on individual trajectories, $D \propto L^2$ when D and L vary along a trajectory. Consequently, Λ_{conf} varies only moderately (see Fig. 2, bottom). This is well mimicked by the slow variations of D at fixed L that we have imposed in numerical trajectories. If $\delta t = \tau_{\text{res}}/3$ exceeds 15 s, we set $\delta t = 15$ s, not to lose too many points at the beginning and the end of the trajectory (see Fig. 2). We eliminate the 18 trajectories that do not satisfy condition (5), as well as those that were qualified of “slow or directed diffusion” in Ref. [4], because their MSD were more correctly fitted by the corresponding theoretical equations. We are left with 67 trajectories.

First of all, we check that $\bar{\Lambda} \gg 4$ on all profiles. This confirms that all trajectories are confined. From the value of τ_{res} , we estimate the expected number of jumps, *if the trajectories were correctly described by a fence or corral model*, namely, $(T - \delta t)/\tau_{\text{res}}$. Then, we count the detected jumps. An example is provided in Fig. 2 (bottom). We find that the average ratio of detected jumps to the ones expected with fence or corral models is only $\sigma_{\text{exp}} = 16.4\%$, where we expected more than 55%. The histogram in Fig. 3 gives greater details. Therefore, as already concluded using independent arguments in Ref. [4], a fence or corral model *is not able to account alone for experimental observations*.

We clearly see that two populations of receptors emerge in the histogram. The first population (empty bars) contains 19 trajectories, of average detection ratio $\sigma'_{\text{exp}} = 58\%$, the detected jumps of which can perfectly be accounted for by a fence or picket model. The second population (shaded bar) concerns 48 trajectories where *we do not detect any jump*.

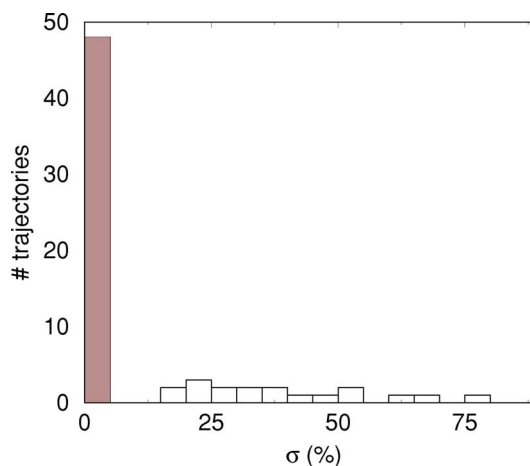


FIG. 3. (Color online) Histogram: ratios of detected jumps to the ones expected in a fence model, on experimental 67 trajectories of μ -opioid receptors [4]. An event at $\sigma=400\%$ is not shown.

Their long-term diffusion *cannot* be explained by any fence or picket model.

We are led to the following original conclusion: hop diffusion probably exists in trajectories of μ -opioid receptors and can satisfyingly explain the long-term diffusive behavior of nearly 30% of the analyzed trajectories. But another mechanism must be invoked to explain long-term diffusion in a majority of cases. This reinforces the need for an alternative model to account for long-term diffusion, as proposed in Ref. [4]. We might even ask if two distinct mechanisms are not independently at work in cells to achieve confinement, and if there would not exist two populations of μ receptors: the first ones confined by fences or pickets and the other ones by long-range inter-protein interactions. Additional experiments will be necessary to test this hypothesis.

We express our gratitude to Ken Jacobson for helpful discussions. We also acknowledge the French Ministry of Research and the CNRS for financial support.

-
- [1] M. J. Saxton and K. Jacobson, *Annu. Rev. Biophys. Biomol. Struct.* **26**, 373 (1997).
- [2] Y. Chen, B. Chang, and K. Jacobson, *Lipids* **39**, 115 (2004).
- [3] K. Jacobson, E. D. Sheets, and R. Simon, *Science* **268**, 1441 (1995).
- [4] F. Dumas, N. Destainville, C. Millot, A. Lopez, D. S. Dean, and L. Salomé, *Biophys. J.* **84**, 356 (2003).
- [5] D. Choquet and A. Triller, *Nat. Rev. Neurosci.* **4**, 251 (2003).
- [6] K. Suzuki, K. Ritchie, E. Kajikawa, T. Fujiwara, and A. Kusumi, *Biophys. J.* **88**, 3659 (2005).
- [7] B. C. Lagerholm, G. E. Weinreb, and N. L. Thompson, *Annu. Rev. Phys. Chem.* **56**, 309 (2005).
- [8] A. Kusumi, Y. Sako, and M. Yamamoto, *Biophys. J.* **65**, 2021 (1993).
- [9] T. Fujiwara, K. Ritchie, H. Murakoshi, K. Jacobson, and A. Kusumi, *J. Cell Biol.* **157**, 1071 (2002).
- [10] R. Simson, E. D. Sheets, and K. Jacobson, *Biophys. J.* **69**, 989 (1995).
- [11] A. Kusumi, C. Nakada, K. Ritchie, K. Murase, K. Suzuki, H. Murakoshi, R. S. Kasai, J. Kondo, and T. Fujiwara, *Annu. Rev. Biophys. Biomol. Struct.* **34**, 351 (2005).
- [12] J. Rudnick and G. Gaspari, *Elements of the Random Walk* (Cambridge University Press, Cambridge, England, 2004).
- [13] J. Rudnick and G. Gaspari, *J. Phys. A* **19**, L191 (1986).